European Journal of Nuclear Medicine and Molecular Imaging (2019) 46:1672–1677
https://doi.org/10.1007/s00259-019-04329-0

ORIGINAL ARTICLE

Ultrafast bone scintigraphy scan for detecting bone metastasis using a CZT whole-body gamma camera

Tomohiko Yamane[1,2] · Atsushi Kondo[3,4] · Masafumi Takahashi[3] · Yuuki Miyazaki[3] · Toshihiko Ehara[3] · Kenji Koga[3] · Ichiei Kuji[1] · Ichiro Matsunari[2]

Received: 4 October 2018 / Accepted: 2 April 2019 / Published online: 1 May 2019

Abstract

Purpose To evaluate the feasibility of short whole-body bone scan acquisition times using a novel gamma camera with cadmium-zinc-telluride (CZT) semiconductor detectors.

Methods We retrospectively enrolled 78 consecutive patients with prostate cancer who underwent bone scintigraphy using a whole-body gamma camera with CZT detectors. After acquisition of list-mode data with 180 s per bed position, anterior and posterior whole-body images were reconstructed using the first 5%, 10%, 25%, 50%, 75% and 100% of the list-mode data. Two experienced nuclear medicine physicians interpreted the images, and interrater agreement and the diagnostic value of the images were determined. Quantitative artificial neural network (ANN) values, bone scan indexes (BSI) and hotspot numbers (HsN) were also calculated by automated diagnostic software.

Results Excellent interrater reliabilities of the visual assessments were obtained for the 100%, 75%, 50%, and 25% images (κ = 0.88, 0.88, 0.88 and 0.88, respectively). The 5% images also showed high diagnostic value (sensitivity 0.94, specificity 0.84 and accuracy 0.86). Intraclass correlation coefficients (ICC) between the 100% images and the reduced acquisition time images were evaluated in quantitative analyses, and excellent correlations were observed for ANN value in the 75% images (ICC 0.77), for BSI in all the reduced acquisition time images (75%, 50%, 25%, 10% and 5%; ICC 0.99, 0.99, 0.99, 0.96 and 0.75, respectively), and for HsN in the 75%, 50%, 25% and 10% images (ICC 0.99, 0.99, 0.98 and 0.90, respectively).

Conclusion Whole-body gamma cameras with CZT detectors have the potential to reduce image acquisition times and the dose of radioisotope injected for bone scans.

Keywords Bone scan · Cadmium-zinc-telluride (CZT) · Gamma camera · Bone metastasis of prostate cancer · Ultrafast scan

Introduction

Recent advances including anticancer and radionuclide therapy have provided many options for the treatment of bone metastasis [1–3]. Precise evaluation of bone activity is required to determine the suitability of these treatments and to evaluate treatment responses. In addition to morphological procedures such as plain radiography, computed tomography (CT) and magnetic resonance imaging, metabolic procedures such as bone scan with ^{99m}Tc-labelled compounds have been widely used to evaluate bone disorders. In recent years, there has been progress in objective and quantitative methods of analysis of planar scintigraphy and single photon emission CT (SPECT) bone scans [4–6]. Bone scans with automated diagnostic software have frequently been used to monitor

✉ Tomohiko Yamane
yamane_t@saitama-med.ac.jp

1 Department of Nuclear Medicine, Saitama Medical University International Medical Center, 1397-1 Yamane, Hidaka 350-1298, Japan

2 Division of Nuclear Medicine, Department of Radiology, Saitama Medical University Hospital, 38 Moro-Hongo, Moroyama 350-0495, Japan

3 Department of Central Radiological Technology, Saitama Medical University Hospital, 38 Moro-Hongo, Moroyama 350-0495, Japan

4 Department of Radiological Technology, Graduate School of Health Science, Tokyo Metropolitan University, 7-2-10 Higashi-Oku, Arakawa-ku, Tokyo 116-8551, Japan

bone activity, especially in patients with prostate cancer that often leads to osteoblastic bone metastasis [2, 3].

In patients undergoing multiple bone scans, radiation exposure should be minimized. In addition, shorter scan times are preferable to allow facilities to deal with as many tasks as possible with limited resources. Gamma cameras with semiconductor detectors, compared with conventional scintillation detectors, have the potential to reduce acquisition times and injection doses because of their high energy and spatial resolution. Several studies have shown that SPECT with cadmium zinc telluride (CZT) semiconductor detectors, designed for cardiac imaging, provides ultrafast data acquisition [7–10]. Recently, a new whole-body scanner with CZT semiconductor detectors has become commercially available [11]. Although this scanner also has the potential to reduce scan times and injection doses, little has been reported on its clinical efficacy.

We hypothesized that the novel whole-body CZT gamma camera may also be able to reduce the scan times or injection doses of radiotracer. The aim of this study was to evaluate the feasibility of whole-body bone scans with short acquisition times using the gamma camera with CZT semiconductor detectors.

Materials and methods

Patients

The study was approved by the institutional review board and the need for written informed consent for this retrospective analysis was waived (registration number 18079.01). A total of 78 consecutive male patients (age range 57 to 87 years, median 73 years) who underwent bone scintigraphy for the detection of bone metastasis from prostate cancer were enrolled from July 2017 to March 2018.

Bone scan

Approximately 3 h after intravenous injection of ^{99m}Tc-methylene diphosphonate (^{99m}Tc-MDP), bone scan images were acquired using the novel whole-body SPECT/CT scanner with CZT detectors (Discovery NM/CT 670 CZT; GE Healthcare, Chicago, IL). The median activity of the injection was 759 MBq (range 652–893 MBq) and the median time from injection to image acquisition was 180 min (range 120–200 min). Patients were required to void just before image acquisition. After acquisition of list-mode data with 180 s per bed position using a wide-energy high-resolution collimator, anterior and posterior whole-body images were reconstructed on the workstation (Xeleris 9.0; GE Healthcare) using the first 5%, 10%, 25%, 50%, 75% and 100% of the list-mode data. The energy window for the reconstructions was set at 140 keV ±5.0%. No SPECT or CT data were used in the present study.

Visual analysis

Images were visually dichotomized into positive or negative for metastasis as interpreted independently by two experienced nuclear medicine physicians (T.Y. with 20 years of experience, and I.M. with 32 years of experience). Cases in which the interpretations of the two reviewers were different were discussed with another experienced nuclear medicine physician (I.K. with 29 years of experience), and the final decisions were made in consensus of the three physicians.

Quantitative analysis

For evaluating the images, artificial neural network (ANN) values, bone scan indexes (BSI) and hotspot numbers (HsN) were calculated using automated analysis software (BONENAVI, version 2.1.7; FUJIFILM Toyama Chemical) that uses the same algorithm, except for the database, as the software EXINIbone^{BSI} (EXINI Diagnosis, Lund, Sweden) [12]. The ANN value, an indicator of malignancy, is a value between 0 and 1, with an ANN value of 1 indicating a high probability of malignancy [13]. BSI is the bone metastasis mass expressed as a percentage of the total tumour mass [14]. A BSI of 0% indicates no malignant lesions. HsN is the number of lesions considered to have a high probability of metastasis by the software. The automated software initially performed the segmentation of the skeletons, and the segmentation images are shown. The images were then evaluated visually to ensure that the segmentation had been correctly performed.

Statistics

For the visual analysis, interrater agreement between the two interpreters was evaluated by Cohen's kappa coefficient (κ). Based on the consensus read, sensitivities, specificities and accuracies were calculated for the short acquisition time images by setting the 100% images as the reference. For the quantitative analysis, the correlations for the ANN values, BSI and HsN between the 100% image and each of the time-reduced images were statistically evaluated using the intraclass correlation coefficient (ICC). For interpretation of κ and the ICC, the following categories were used: <0.40, poor; 0.40 to 0.59, fair; 0.60 to 0.74, good; and 0.75 to 1.00, excellent. Bland-Altman plots were also used to evaluate the differences. Data were analysed using IBM SPSS Statistics, version 25 (IBM, Armonk, NY, USA). Values expressed with plus/minus indicate the means ± standard deviation.

Results

The average count of the anterior and posterior reconstructed whole-body 100% images was $2.10 \pm 0.46 \times 10^6$. Representative cases are shown in Fig. 1.

Qualitative analysis

The results of the qualitative visual assessment are summarized in Table 1. Excellent agreement between the interpretations of the two experienced nuclear medicine physicians was observed for the 100% images and the 75%, 50%, and 25% images. Good agreement was observed for the 10% images and fair agreement for the 5% images. Sensitivity, specificity and accuracy were 1.00 for the 75% and 50% images, indicating that the interpretations of these short-acquisition time images were the same as those of the 100% images. Sensitivities were 0.94 for the 25%, 10% and 5% images. Specificities decreased gradually from 0.98 for the 25% images to 0.84 for the 5% images. Accuracy also decreased from 0.97 for the 25% images to 0.86 for the 5% images.

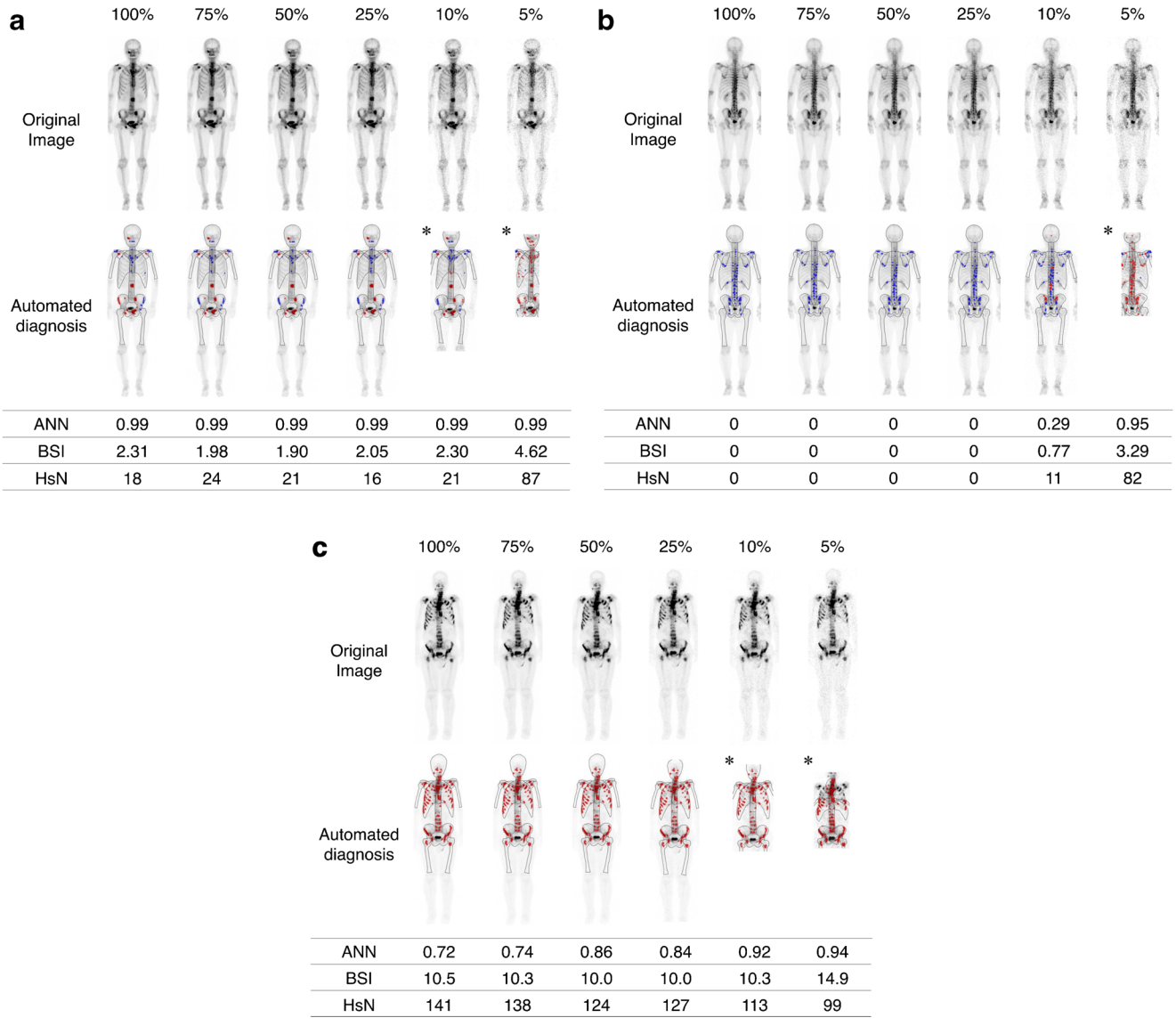

	100%	75%	50%	25%	10%	5%
ANN	0.99	0.99	0.99	0.99	0.99	0.99
BSI	2.31	1.98	1.90	2.05	2.30	4.62
HsN	18	24	21	16	21	87

	100%	75%	50%	25%	10%	5%
ANN	0	0	0	0	0.29	0.95
BSI	0	0	0	0	0.77	3.29
HsN	0	0	0	0	11	82

	100%	75%	50%	25%	10%	5%
ANN	0.72	0.74	0.86	0.84	0.92	0.94
BSI	10.5	10.3	10.0	10.0	10.3	14.9
HsN	141	138	124	127	113	99

Fig. 1 Representative cases: **a** anterior images in a patient with nondiffuse multiple bone metastases; **b** posterior images in a patient without any bone metastasis; **c** anterior images in a patient with diffuse bone metastases (*top rows* original images, *bottom rows* calculated images constructed by the automated software). Major bones are outlined in black for quality check. Uptake considered benign is indicated in *blue*, uptake considered malignant is indicated in *red*. The ANN value, BSI and HsN for each reconstructed image are also shown. *Asterisks* indicate the images for which skeletal segmentation was not successful (**a**, **c** 10% images; all 5% images). Although the shorter acquisition images are rougher, the diagnostic quality of the 25% images appears to have been retained as well as the quantitative values. *ANN* artificial neural network, *BSI* bone scan index, *HsN* hotspot number

Table 1 Qualitative visual assessment of short-acquisition images

	100% images	75% images	50% images	25% images	10% images	5% images
Rate of agreement (%)[a]	96.2	96.2	96.2	96.2	87.2	77.0
Kappa[a]	0.88 (0.76–1.00)	0.88 (076–1.00)	0.88 (0.76–1.00)	0.88 (0.76–1.00)	0.66 (0.47–0.84)	0.48 (0.30–0.66)
Sensitivity[b]	–	1.00 (1.00–1.00)	1.00 (1.00–1.00)	0.94 (0.90–0.99)	0.94 (0.90–0.99)	0.94 (0.90–0.99)
Specificity[b]	–	1.00 (1.00–1.00)	1.00 (1.00–1.00)	0.98 (0.96–1.00)	0.95 (0.90–0.99)	0.84 (0.76–0.91)
Accuracy[b]	–	1.00 (1.00–1.00)	1.00 (1.00–1.00)	0.97 (0.94–1.00)	0.95 (0.91–0.99)	0.86 (0.79–0.93)

Values in parentheses are 95% confidence intervals

[a] Rate of agreement and kappa index are based on the interpretations of two independent readers

[b] Sensitivity, specificity and accuracy are based on a consensus read.

Quantitative analysis

For the 100% images, the average ANN value, BSI and HsN were 0.33 ± 0.37, 1.01 ± 2.35 and 10.2 ± 25.9. Although all the quantitative values could be calculated for all the reconstructed images in all cases, segmentation mismatches or deficits of parts of the image in the image reports of the automated software were observed in 17 out of 78 cases for the 10% images (21.8%) and in all the cases for the 5% images (100%).

The Bland-Altman plots of the ANN value, BSI and HsN are shown in Fig. 2. For the ANN value, excellent correlations were observed between the 100% images and the 75% images, and good correlations were observed between the 100% images and the 50%, 25% and 10% images. For BSI, all the ICCs, including those between the 100% images and the 5% images, showed excellent correlations. For the HsN, excellent correlations were observed between the 100% images and the 75%, 50%, 25% and 10% images.

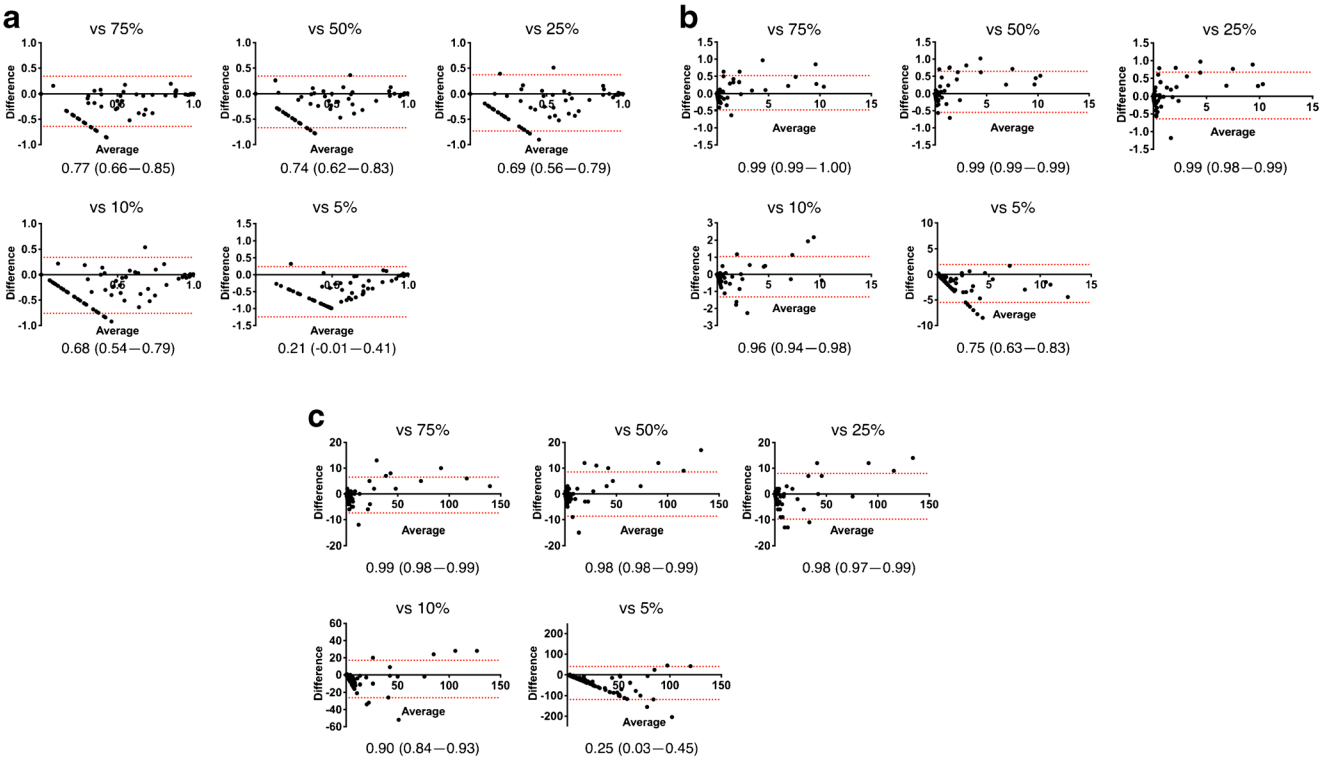

Fig. 2 Bland-Altman plots of ANN values (**a**), BSI (**b**) and HsN (**c**). ICCs are shown together with 95% confidence intervals in parentheses. The averages and the differences between the 100% images and the short-acquisition time images are shown. The *red horizontal dotted lines* indicate the upper and lower 95% limits of agreement. Some systematic linear relationships in the clusters of points in the bottom left of the plots indicate cases in which the whole value of the 100% images is zero and another value in a reduced acquisition time image is relatively high. *ANN* artificial neural network, *BSI* bone scan index, *HsN*: hotspot number, *ICC* intraclass correlation coefficient

Discussion

This study evaluated the feasibility of whole-body bone scans with short acquisition times using a novel gamma camera with CZT semiconductor detectors. In the visual evaluation, excellent interrater agreements were observed for the 25% images and even the 5% images showed high diagnostic value. In the quantitative analysis, BSI showed excellent correlations between the original 100% images and the short acquisition time images, including the 5% images. Therefore, whole-body bone scanning with a CZT camera has the potential to reduce scan times and the dose of radioisotope injected for bone scintigraphy. In the automated software analysis, segmentation mismatches or deficits in parts of the images were observed in 21.8% of the 10% images and in 100% of the 5% images. These images must be considered to lack credibility even though their quantitative values could be calculated. Therefore, a scan time of approximately 25% can be considered as the minimum. This percentage indicates a radioactivity dose of 190 MBq, or an acquisition time per bed position of 45 s (i.e. 3.75 min for the five bed positions to the cover whole body).

We focused on patients with prostate cancer in this study. Bone metastasis of prostate cancer is unique because the resulting tumours tend to be osteoblastic rather than osteolytic [15], and the uptake observed on bone scintigraphy tends to increase significantly [16]. The characteristics of bone scans and their quantitative values are known to be different among different types of primary malignancies [17]. Therefore, further research is needed before this method can be used in the other conditions.

Although ultrashort acquisitions provided images of high diagnostic value by visual assessment, ultrashort acquisitions may not be appropriate for initial diagnosis. While the ANN value is an indicator of malignancy [13], the concordance for the ANN value is generally lower than that for the BSI. Using an ANN of 0.5 or more to define malignancy has been shown to provide a sensitivity of 82% and a specificity of 83% in the detection of bone metastasis [18]. Variation in the ANN value can reduce its high diagnostic value. The ANN values for the 100% and 75% images showed excellent agreement (ICC 0.77). However, lower agreements were observed for the shorter acquisition time images. Therefore, the injected dose or acquisition time should be at least 75% of the original values for initial diagnosis. On the other hand, the concordance for the BSI was excellent even in the 5% images. This indicates that the BSI from ultrashort acquisition time images could potentially be used to monitor treatment responses. The BSI indicates the fraction of the bone that is involved by the tumour [19] and is considered a good biomarker of bone metastasis from prostate cancer [14, 19, 20]. Therefore, repeated short acquisition time or low-dose bone scans could be used for follow-up in this condition.

Conclusion

We evaluated the feasibility of whole-body bone scans with short acquisition times using the novel gamma camera with CZT semiconductor detectors. Visual assessment of the ultrafast scan images was highly diagnostic, and the quantitative values showed excellent correlations between the original 100% images and the ultrafast scan images. Whole-body CZT gamma cameras have the potential to reduce image acquisition times and the dose of radioisotope injected for evaluating the BSI of bone scans in patients with bone metastasis of prostate cancer.

Compliance with ethical standards

Conflicts of interest None.

Ethical approval All procedures performed in studies involving human participants were in accordance with the ethical standards of the institutional review board and with the principles of the 1964 Declaration of Helsinki and its later amendments or comparable ethical standards.

Informed consent The need for informed consent was waived by the Review Board of Saitama Medical University, due to the retrospective nature of this study.

References

1. Logothetis C, Morris MJ, Den R, Coleman RE. Current perspectives on bone metastases in castrate-resistant prostate cancer. Cancer Metastasis Rev. 2018;37:189–96. https://doi.org/10.1007/s10555-017-9719-4.
2. Bieth M, Kronke M, Tauber R, Dahlbender M, Retz M, Nekolla SG, et al. Exploring new multimodal quantitative imaging indices for the assessment of osseous tumor burden in prostate cancer using (68)Ga-PSMA PET/CT. J Nucl Med. 2017;58:1632–7. https://doi.org/10.2967/jnumed.116.189050.
3. Fosbol MO, Petersen PM, Kjaer A, Mortensen J. (223)Ra therapy of advanced metastatic castration-resistant prostate cancer: quantitative assessment of skeletal tumor burden for prognostication of clinical outcome and hematologic toxicity. J Nucl Med. 2018;59:596–602. https://doi.org/10.2967/jnumed.117.195677.
4. Anand A, Morris MJ, Kaboteh R, Reza M, Tragardh E, Matsunaga N, et al. A preanalytic validation study of automated bone scan index: effect on accuracy and reproducibility due to the procedural variabilities in bone scan image acquisition. J Nucl Med. 2016;57:1865–71. https://doi.org/10.2967/jnumed.116.177030.
5. Anand A, Morris MJ, Kaboteh R, Bath L, Sadik M, Gjertsson P, et al. Analytic validation of the automated bone scan index as an imaging biomarker to standardize quantitative changes in bone scans of patients with metastatic prostate cancer. J Nucl Med. 2016;57:41–5. https://doi.org/10.2967/jnumed.115.160085.
6. Yamane T, Kuji I, Seto A, Matsunari I. Quantification of osteoblastic activity in epiphyseal growth plates by quantitative bone SPECT/CT. Skelet Radiol. 2018;47:805–10.
7. Mouden M, Timmer JR, Ottervanger JP, Reiffers S, Oostdijk AH, Knollema S, et al. Impact of a new ultrafast CZT SPECT camera for myocardial perfusion imaging: fewer equivocal results and lower

radiation dose. Eur J Nucl Med Mol Imaging. 2012;39:1048–55. https://doi.org/10.1007/s00259-012-2086-z.
8. Buechel RR, Herzog BA, Husmann L, Burger IA, Pazhenkottil AP, Treyer V, et al. Ultrafast nuclear myocardial perfusion imaging on a new gamma camera with semiconductor detector technique: first clinical validation. Eur J Nucl Med Mol Imaging. 2010;37:773–8. https://doi.org/10.1007/s00259-009-1375-7.
9. Cochet H, Bullier E, Gerbaud E, Durieux M, Godbert Y, Lederlin M, et al. Absolute quantification of left ventricular global and regional function at nuclear MPI using ultrafast CZT SPECT: initial validation versus cardiac MR. J Nucl Med. 2013;54:556–63. https://doi.org/10.2967/jnumed.112.110577.
10. Herzog BA, Buechel RR, Katz R, Brueckner M, Husmann L, Burger IA, et al. Nuclear myocardial perfusion imaging with a cadmium-zinc-telluride detector technique: optimized protocol for scan time reduction. J Nucl Med. 2010;51:46–51. https://doi.org/10.2967/jnumed.109.065532.
11. Ljungberg M, Pretorius PH. SPECT/CT: an update on technological developments and clinical applications. Br J Radiol. 2018;91:20160402. https://doi.org/10.1259/bjr.20160402.
12. Koizumi M, Wagatsuma K, Miyaji N, Murata T, Miwa K, Takiguchi T, et al. Evaluation of a computer-assisted diagnosis system, BONENAVI version 2, for bone scintigraphy in cancer patients in a routine clinical setting. Ann Nucl Med. 2015;29:138–48. https://doi.org/10.1007/s12149-014-0921-y.
13. Nakajima K, Nakajima Y, Horikoshi H, Ueno M, Wakabayashi H, Shiga T, et al. Enhanced diagnostic accuracy for quantitative bone scan using an artificial neural network system: a Japanese multicenter database project. EJNMMI Res. 2013;3:83. https://doi.org/10.1186/2191-219X-3-83.
14. Ulmert D, Kaboteh R, Fox JJ, Savage C, Evans MJ, Lilja H, et al. A novel automated platform for quantifying the extent of skeletal tumour involvement in prostate cancer patients using the bone scan index. Eur Urol. 2012;62:78–84. https://doi.org/10.1016/j.eururo.2012.01.037.
15. Logothetis CJ, Lin SH. Osteoblasts in prostate cancer metastasis to bone. Nat Rev Cancer. 2005;5:21–8. https://doi.org/10.1038/nrc528.
16. Kuji I, Yamane T, Seto A, Yasumizu Y, Shirotake S, Oyama M. Skeletal standardized uptake values obtained by quantitative SPECT/CT as an osteoblastic biomarker for the discrimination of active bone metastasis in prostate cancer. Eur J Hybrid Imaging. 2017;1:2.
17. Isoda T, BaBa S, Maruoka Y, Kitamura Y, Tahara K, Sasaki M, et al. Influence of the different primary cancers and different types of bone metastasis on the lesion-based artificial neural network value calculated by a computer-aided diagnostic system, BONENAVI, on bone scintigraphy images. Asia Ocean J Nucl Med Biol. 2017;5:49–55. https://doi.org/10.22038/aojnmb.2016.7606.
18. Koizumi M, Motegi K, Koyama M, Terauchi T, Yuasa T, Yonese J. Diagnostic performance of a computer-assisted diagnosis system for bone scintigraphy of newly developed skeletal metastasis in prostate cancer patients: search for low-sensitivity subgroups. Ann Nucl Med. 2017;31:521–8. https://doi.org/10.1007/s12149-017-1175-2.
19. Imbriaco M, Larson SM, Yeung HW, Mawlawi OR, Erdi Y, Venkatraman ES, et al. A new parameter for measuring metastatic bone involvement by prostate cancer: the bone scan index. Clin Cancer Res. 1998;4:1765–72.
20. Dennis ER, Jia X, Mezheritskiy IS, Stephenson RD, Schoder H, Fox JJ, et al. Bone scan index: a quantitative treatment response biomarker for castration-resistant metastatic prostate cancer. J Clin Oncol. 2012;30:519–24. https://doi.org/10.1200/JCO.2011.36.5791.